

1

UCLA School of Engineering and Applied Science

AD-A213 509

DTIC
ELECTE
OCT 19 1989
S D CS D

Department of Civil Engineering

UCLA-ENG-89-09

**Micromechanics of an Extrusion in
High-Cycle Fatigue With Creep**

The report was sponsored by the Office of Naval Research Through contract
N00014-86-K0153

T.H.Lin
S.R.Lin
X.Q.Wu

UNCLASSIFIED
Approved for public release;
Distribution Unlimited

89 9 19 029

Micromechanics of An Extrusion in

High-Cycle Fatigue With Creep

T.H. Lin* Fellow ASME, S.R. Lin** and X.Q. WU*

Abstract

A most favorably oriented crystal located at a free surface of a f.c.c. polycrystal subject to creep under cyclic tension and compression of high-cycle fatigue is considered. An extrusion in this crystal is shown to be produced by a positive slip in one thin slice "P" and a negative slip in a closely located slice "Q". An initial tensile strain $\epsilon_{\alpha\alpha}^I$ in the thin slice "R" sandwiched between P and Q causes a positive initial shear stress $\tau_{\alpha\beta}^I$ in P and a negative one in Q. It is shown that the extrusion growth causes a tensile strain in R, which can activate a second slip system giving a creep strain with a tensor component $\epsilon_{\alpha\alpha}^c$. It has the same effect as the initial strain $\epsilon_{\alpha\alpha}^I$ in causing this difference in shear stresses in P and Q and gives much additional extrusion growth. The extent of intrusion and extrusion is important in this study of crack initiation.

J	
per ltr	
A-1	

*Department of Civil Engineering, University of California, Los Angeles, Calif. 90024-1593

**The Aerospace Corporation, Structural technology Department, El Segundo, Calif. 90295-2641

Introduction

Single crystal test at room temperature (Taylor, 1938) have shown that, under stress, slip occurs along certain directions on certain planes. Slip, the result of displacement of dislocations, has been found to depend on the resolved shear stress and not on the normal stress on the sliding plane. This dependency of slip on the resolved shear stress, known as Schmid's law, has been shown by Parker, 1961 to hold also under cyclic loadings. Deformation of single crystals at elevated temperatures (Johnson, et al, 1953, 1955) also occurs by slip in primarily the same slip systems that are operative at room temperature. This slip rate was found to depend on the resolved shear stress. This agrees with Gilman's 1969 observation that this dislocation velocity varies with the resolved shear stress.

Following the clue provided by the observation of extrusions and intrusions in fatigue specimens (Forsyth, 1954), a number of distinguished investigators; Mott 1958, Cottrell and Hull 1957, Thompson 1959, McEviley and Machlin 1959, Wood 1956 and others have proposed different theories of fatigue crack initiation. The above early fatigue crack initiation theories primarily consider the paths of dislocation movement without considering the resolved shear stress induced by this movement. This seems to be the main cause for these theories to be not quite satisfactory, as pointed out by Kennedy 1961. Lin and Ito 1969 proposed first quantitative micromechanic theory of fatigue crack initiation. This theory calculates the stress fields produced by slip in fatigue bands and has been shown to agree with nearly all experimental observations (Lin, 1977, 1981). This theory is briefly reviewed here and is applied to the present analysis.

Initial defects always exist in metals and cause an initial stress field. Let the initial resolved shear stress be denoted by τ^I . During loading, when the resolved shear stress in some region reaches the critical shear stress τ^c , slip occurs. After unloading, this slip remains and induces a residual resolved shear stress τ^R . The resolved shear stress due to loading is denoting by τ^A . The total shear stress after reloading is

$$\tau = \tau^I + \tau^R + \tau^A \quad (1)$$

Consider a most favorably oriented crystal at a free surface of a f.c.c. polycrystal as shown in Fig. 1. For an extrusion to start in a thin slice R sandwiched between two slices P and Q, positive shear must occur in P and negative in Q. The initial shear stress field τ^I , favorable for this sequence of slip, clearly is one having positive shear stress in P and negative in Q. Such an initial stress field can be provided by an initial tensile strain $\epsilon_{\alpha\alpha}^I$ in R. This positive $\epsilon_{\alpha\alpha}^I$ can be provided by a row of interstitial dislocation dipoles and a negative $\epsilon_{\alpha\alpha}^I$ by vacancy dislocation dipoles as shown by Lin and Ito 1969.

A tensile loading τ_{22} on the polycrystal (Fig. 1) produces a positive τ^A in the whole crystal. Taking τ^I to be positive in P and negative in Q, we have $\tau^I + \tau^A$ in P reaching the critical shear stress τ^c first; and hence, P slides. Due to the continuity of stress field, slip in P relieves not only the positive shear stress in P but also in Q (Lin and Ito, 1969, Lin 1977). Hence, this slip increases the negative resolved shear stress in Q to cause Q to slide more readily in the reverse loading. The negative slip in Q relieves the negative shear stress not

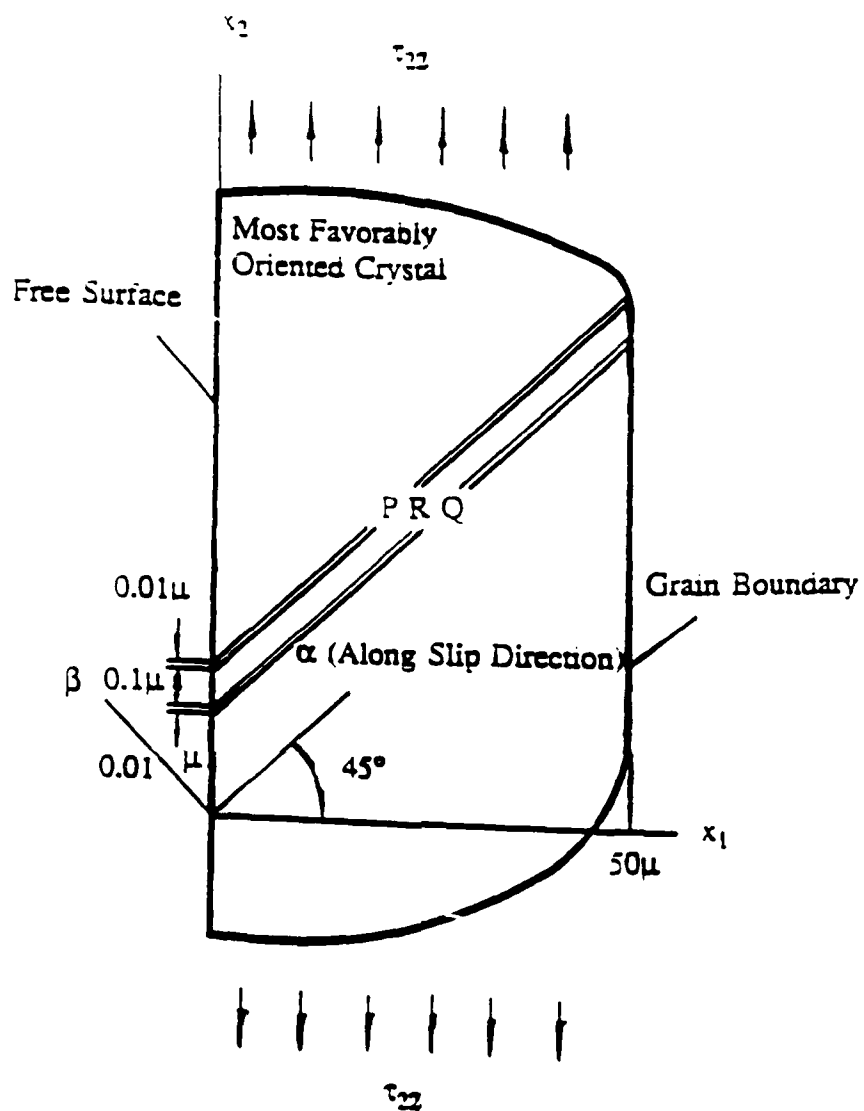


Figure 1. Most Favorably Oriented Crystal at Free surface

only in Q, but also in P, thus causing P more readily to slide in the next forward loading. This process is repeated for every cycle thus providing a natural gating mechanism for a monotonic buildup of local slip strain $\epsilon_{\alpha\beta}^c$ in P and Q, pushing R out of the free surface and starts an extrusion. Interchanging the signs of the initial stresses in P and Q initiates an intrusion instead of an extrusion. This theory is extensively supported by metallurgical observations (Lin, 1977).

Extent of Extrusion

The buildup of this local slip strain $\epsilon_{\alpha\beta}^c$ in P and Q is caused by the positive and negative initial shear stresses $\tau_{\alpha\beta}^I$ which, in turn, is caused by $\epsilon_{\alpha\alpha}^I$ in R. If R were cut out, this free length of R would be longer than the slot cut by an amount referred to as the "static extrusion" (Mughrabi et al, 1983). This $\epsilon_{\alpha\alpha}^I$ causes an initial compression $\tau_{\alpha\alpha}^I$ in R. As the extrusion grows under cyclic loading, the slice R increases in length. This elongation causes the compression to decrease. A question has been raised as to whether the extrusion growth will cease after the extrusion has reached the static extrusion. Lin, et al., 1988 have shown that the residual tensile stress $\tau_{\alpha\alpha}^R$ caused by elongation in R due to extrusion can cause changes of resolved shear stresses in all twelve slip systems. The resolved shear stress in one slip system may reach the critical and slide. The creep strain $\epsilon_{\xi\eta}^c$ caused by slip in this system has a tensor component $\epsilon_{\alpha\alpha}^c$ just like $\epsilon_{\alpha\alpha}^I$ in causing the positive and negative $\tau_{\alpha\beta}^I$, respectively, in P and Q. This secondary slip has been shown by Lin, et al., 1988 to increase greatly the extent of extrusion and intrusion in time-independent slip. This paper shows the this secondary slip also increases this extent of intrusion and extrusion in fatigue with creep.

Residual Stress Field Caused by Creep Strain

The creep rate depends on the resolved shear stress τ which is given in Eq. 1. as the sum of the initial, applied and residual shear stresses. To calculate τ , the analogy of creep strain and applied force is applied. It has been shown that the equivalent body force per unit volume along x_i - axis due to creep strain ϵ_{ij}^c is

$$\underline{F}_i = -(\lambda \delta_{ij} \epsilon_{kk,i} + 2G \epsilon_{ij,j}) \quad (2)$$

where λ and G are Lamé's constants and δ_{ij} is the Kronecker delta. The repetition of subscript denotes summation and the subscript after comma denotes differentiation, with respect to the coordinate variable. The equivalent surface force per unit area along the x_i - axis also has been shown as

$$\underline{S}_i = (\lambda \epsilon_{kk} \delta_{ij} + 2G \epsilon_{ij}) v_j \quad (3)$$

where v_j is the cosine of the angle between the exterior normal to the surface and the x_j - axis.

From a given ϵ_{ij}^c , we obtain \underline{F}_i and \underline{S}_i from Eqs. (2) and (3). Then we apply this \underline{F}_i and \underline{S}_i to the body and obtain the strain distribution ϵ_{ij} in this body by elastic solution. The residual stress field in this body is then

$$\tau_{ij}^R = \lambda \delta_{ij} \epsilon_{kk} + 2\mu \epsilon_{ij} - \lambda \delta_{ij} \epsilon_{kk}^c - 2\mu \epsilon_{ij}^c \quad (4)$$

This analogy becomes Duhamel's analogy for thermal stress (Lin, 1968), if the creep strain ϵ_{ij}^c is replaced by thermal strain ϵ_{ij}^T .

The lengths of the strips P, Q and R along the x_3 -direction are much larger than the thickness; the thickness also is much smaller than their inclined lengths shown in Fig. 1. Hence, strains in the major central portion of the strips are taken to be of generalized plane strain, i.e.

$$u_i = u_i(x_1, x_2) \quad i = 1, 2, 3 \quad (5)$$

This gives

$$\tau_{ij} = 2\mu \left[\frac{\nu}{1-2\mu} \delta_{ij} \theta + \frac{1}{2} (u_{i,j} + u_{j,i}) \right] \quad (6)$$

where $\theta = u_{1,1} + u_{2,2}$ and ν is Poisson's ration. Substitution of the expression into the conditions of equilibrium yields

$$\nabla^2 u_\alpha + \frac{1}{1-2\mu} \frac{\partial \theta}{\partial x_\alpha} + \frac{F_\alpha}{G} = 0, \quad \alpha = 1, 2 \quad (7)$$

and

$$\nabla^2 u_3 + \frac{F_3}{G} = 0 \quad (8)$$

where

$$\nabla^2 = \frac{\partial^2}{\partial x_1^2} + \frac{\partial^2}{\partial x_2^2}$$

where F_α and F_3 can be either the applied forces or the equivalent forces.

The above two equations (7) and (8) are not coupled and can be solved separately. Lin and Lin 1974 and Lin, et al., 1988 have shown the solution of this stress field caused by

F_α by using Airy's stress functions. The solution of the displacement fields and then the stress fields caused by F_3 also has been shown by Lin, et al., 1988. Consequently the stress fields caused by the equivalent forces due to creep strain can readily be calculated.

The twelve slip systems of a f.c.c. crystal are shown in Fig. 2. The most favorable slip system in the most favorably oriented crystal making 45° with the direction of loading is identified with a_2 (Fig. 2). During fatigue loading, this buildup of large local creep shear strain $\epsilon''_{\alpha\beta}$ in P and Q causes R to elongate, inducing an appreciable direct stress $\tau_{\alpha\alpha}$. It has been shown by Lin, et al., (1988) that there are four slip systems c_1 , c_3 , d_1 and d_2 equally favorable under $\tau_{\alpha\alpha}$. Among the four c_3 is the most favorable under this applied load τ_{22} . Hence, c_3 is considered to be active in R.

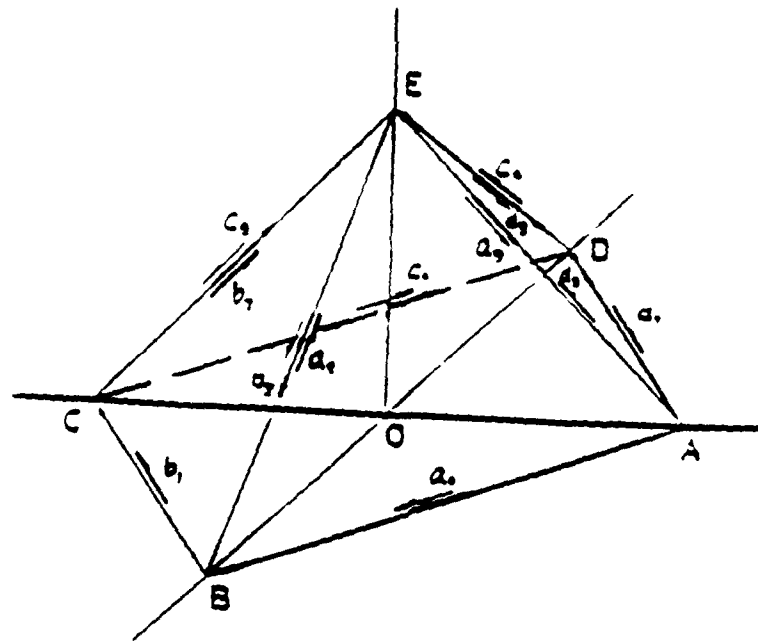


Figure 2. Crystallographic Directions of a f.c.c. Crystal

The normal to the slip plane β and the slip direction α of the slip system a_2 lie in the $x_1 x_2$ plane. The equivalent forces \underline{F}_α caused by slip $\epsilon_{\alpha\beta}^c$ in the a_2 - slip system are in this plane. Hence plane strain solution satisfying the differential equation (7) was used (Lin and Lin 1974). However the slip direction ξ and the normal to the slip plane η of the c_3 slip system are not in the $x_1 x_2$ - plane. The equivalent forces caused by slip $\epsilon_{\xi\eta}^c$ in the c_3 slip system does not lie in the $x_1 x_2$ - plane. Hence the equivalent force has a component \underline{F}_3 . Then the stress fields caused by the components \underline{F}_3 lying in the plane are solved by Eq. 7 and those caused by the component \underline{F}_3 are solved by Eq. 8. (Lin, et al., 1988). This shows how this residual stress caused by creep in the primary slip system $\epsilon_{\alpha\beta}^c$ and those in the secondary slip system $\epsilon_{\xi\eta}^c$ are analytically calculated.

Numerical Calculations

The dimensions of the most favorably oriented crystal at the free surface of a polycrystal of pure aluminum are shown in Fig. 1. The thickness in P and Q is 0.01μ , and the thickness in R is 0.1μ along the x_2 direction. As shown in Fig. 4, the initial shear stress in P, Q is taken to vary linearly from 0 at the interior boundary to $1.1 \times 10^4 Pa$ (1.6 psi) at the free surface. This is expressed as

$$\tau'_{\alpha\beta}(\alpha) = 1.1 \times 10^4 \left(1 - \frac{\alpha}{50\sqrt{2}}\right)$$

From equilibrium conditions

$$\frac{0.1}{\sqrt{2}} \tau'_{\alpha\alpha}(\alpha) = -2 \int_0^\alpha \tau'_{\alpha\beta}(s) ds = -2.2 \times 10^4 \left(\alpha - \frac{\alpha^2}{100 \times \sqrt{2}}\right)$$

$$\epsilon'_{\alpha\alpha}(\alpha) = \frac{-(1 - \nu^2)}{E} \tau_{\alpha\alpha} = 0.412 \times 10^{-5} \left(\alpha - \frac{\alpha^2}{100 \times \sqrt{2}} \right)$$

The static extrusion is then

$$\int_0^{50\sqrt{2}} \epsilon'_{\alpha\alpha}(\alpha) d\alpha = 0.687 \times 10^{-2}$$

The creep strain $\epsilon_{\alpha\beta}^c$ at this free surface corresponding to the above static extrusion is 0.486.

The single crystal creep property is taken from tests at 204.4°C (400°F) performed by Johnson et al, 1953, 1955 and is represented approximately by a linear relation (Lin and Lin, 1978, 1980).

$$\dot{\epsilon}_{\alpha\beta}^c = 3.26 \times 10^{-7} [\tau_{\alpha\beta} - 1.3167 \times 10^6 \text{ N/m}^2 (190.1 \text{ psi})] / \text{min}$$

where the dot on top denotes the time derivative and $\tau_{\alpha\beta}$ is the resolved shear stress in N/m^2 in the active slip system. Creep strain is highly localized in slip bands. The creep rate in this band is much higher than the average rate of the whole crystal and is assumed to be 1000 times that of the crystal giving

$$\dot{\epsilon}_{\alpha\beta}^c = 3.26 \times 10^{-4} (\tau_{\alpha\beta} - 1.3167 \times 10^6 \text{ N/m}^2) / \text{min} \quad (9)$$

Referring to Fig.1, the thin strips P, Q and R are divided along their lengths into thin parallelogram grids. For numerical calculation, the creep strain in each grid is assumed to be constant. Hence, there is no creep strain gradient and no equivalent body force in each grid. However each grid is subject to a set of equivalent surface forces on the boundary. The average residual resolved shear stress in the i th grid caused by constant creep strain $\epsilon_{\alpha\beta}^c$ in the j th grid or $\epsilon_{\xi\eta}^c$ in the k th grid was then calculated using the generalized plane strain semi-infinite

solid solution given by Eqs. 7 and 8 and is denoted by $-C(i, \alpha\beta; j, \alpha\beta)$ or $-C(i, \alpha\beta; k, \xi\eta)$.

With $\epsilon_{\alpha\beta}^c$ occurring only in P, Q and $\epsilon_{\xi\eta}^c$ in R, the residual resolved shear stress in the i th grid due to creep strain $\epsilon_{\alpha\beta}^c$ and $\epsilon_{\xi\eta}^c$ is then written as

$$\begin{aligned}\tau_{\alpha\beta,i}^R &= -C(i, \alpha\beta; j, \alpha\beta)\epsilon_{\alpha\beta,i}^c - C(i, \alpha\beta; k, \xi\eta)\epsilon_{\xi\eta,k}^c \\ \tau_{\xi\eta,i}^R &= -C(i, \xi\eta; j, \alpha\beta)\epsilon_{\alpha\beta,j}^c - C(i, \xi\eta; k, \xi\eta)\epsilon_{\xi\eta,k}^c\end{aligned}\quad (10)$$

The repetition of subscript "j" denotes summation covering all grids with $\epsilon_{\alpha\beta}^c$ and "k" summation covering all grids with $\epsilon_{\xi\eta}^c$. The resolved shear stress in the i th grid is written as

$$\begin{aligned}\tau_{\alpha\beta,i} &= \tau_{\alpha\beta,i}^I + \tau_{\alpha\beta,i}^A + \tau_{\alpha\beta,i}^R \\ \tau_{\xi\eta,i} &= \tau_{\xi\eta,i}^I + \tau_{\xi\eta,i}^A + \tau_{\xi\eta,i}^R\end{aligned}\quad (11)$$

From Eqs. 9 through 11 we can write

$$\begin{aligned}\dot{\epsilon}_{\alpha\beta,i}^c &= 3.26 \times 10^{-4}(\tau_{\alpha\beta,i} - 1.3167 \times 10^6 N/m^2 (190.1 \text{ psi})/\min \\ &= 3.26 \times 10^{-4}[\tau_{\alpha\beta,i}^I + \tau_{\alpha\beta,i}^A - C(i, \alpha\beta; j, \alpha\beta)\epsilon_{\alpha\beta,j}^c \\ &\quad - C(i, \alpha\beta; k, \xi\eta)\epsilon_{\xi\eta,k}^c - 1.3167 \times 10^6 N/m^2 (190.1 \text{ psi})]\end{aligned}\quad (12)$$

A similar equation can be written for $\dot{\epsilon}_{\xi\eta,i}^c$.

From the above, the creep strain rates in grids with resolved shear stress greater than this critical $1.3167 \times 10^6 N/m^2$ (190.1 psi) can be determined.

Write Eq. 12 in matrix form

$$\{\dot{\epsilon}\} = [A]\{\epsilon\} + \{B(\tau)\} \quad (13)$$

subject to the initial condition $\{\epsilon(t_o)\} = \{\epsilon_o\}$. where

$$B_i = 3.26 \times 10^{-4}(\tau_{\alpha\beta_i}^I + \tau_{\alpha\beta_i}^A - 1.316 \times 10^6 N/m^2) \quad (14)$$

The series solution of Eq. 13 is given by Frazer et al, 1963. The complementary solution of Eq. 13 is given as

$$\begin{aligned} \{\epsilon_c\} &= e^{[A](t-t_o)}\{\epsilon_o\} \\ &= \{[I] + [A](t-t_o) + \cdots + \frac{1}{p!}[A]^p(t-t_o)^p + \cdots\}\{\epsilon_o\} \end{aligned} \quad (15)$$

where ϵ_o is this creep strain at t_o , e , the base of the natural logarithm, and $[I]$ is the identify matrix. The particular solution is obtained by multiplying Eq. 13 by $e^{-[A]t}$. This gives

$$\frac{d}{dt}(e^{-[A]t}\{\epsilon_p\}) = e^{-[A]t}\{B(\tau)\}$$

and

$$\{\epsilon_p\} = e^{+[A]t} \int_{t_o}^t e^{-[A](s-t)} \{B(s)\} ds$$

The cyclic loading is taken to be rectangular: i.e., tension and compression are applied instantaneously and remain constant during each half cycle.

$$\{\epsilon_p\} = -\{[I] - e^{[A](t-t_o)}\}[A]^{-1}\{B\}$$

$$\begin{aligned} \{\epsilon_p\} = & \{I(t - t_o) + \frac{1}{2!}[A](t - t_o)^2 + \dots + \frac{1}{p!}[A]^{p-1}(t - t_o)^p \\ & + \dots\}\{B\} \end{aligned} \quad (16)$$

To calculate the creep strain distribution in a given time interval 0 to T. This interval is divided into N steps with $\Delta t = T/N$. The Δt is chosen to be small enough, so the maximum eigenvalue of $[A]\Delta t$ is less than unity. Then the matrix $[A]^n (t - t_o)^n$ approaches a zero matrix as "n" approaches infinity. The series solution of Eqs. 15 and 16 will converge.

For each time step Δt , take the first p-terms of $\{\epsilon_c\}$ and $\{\epsilon_p\}$ to obtain the creep strains. The smaller the Δt and the more terms p used, the more accurate will be the results. In the previous work (Lin and Lin, 1979, 1982), the creep strain rate was assumed to be constant in Δt . The solution corresponds to $p = 1$. It has been found that using this series solution reduces the numerical calculation by more than six times for the same accuracy in evaluating the creep strain distributions. In the present example, the magnitude of applied load was $2.7326 \times 10^6 \text{ N/mm}^2$ (380psi) giving $\tau^A = 1.366 \times 10^6 \text{ N/m}^2$ (190psi). Two loading frequencies were calculated; one is 0.345 cycles/min and the other is 345 cycle/min. In the high frequency loading the half period was equally divided into ten time increments and three terms in the series solution were used. The creep strain in the second slip system $\epsilon_{\xi\eta}^c$ in R versus the distance from the free surface at different cycles of loading under a frequency of 345 cycles per minute was calculated and is shown in Fig. 3. The creep strain $\epsilon_{\xi\eta}^c$ in the second slip system causes some $\epsilon_{\alpha\alpha}^c$ which in turn cause additional positive $+\tau_{\alpha\beta}^R$ in P and negative $-\tau_{\alpha\beta}^R$ in Q. The creep rate in P and Q depends on the sum of the initial and the resi-

dual shear stresses $\tau_{\alpha\beta}^I + \tau_{\alpha\beta}^R$ in P and Q. This sum at different stages of loading is shown in Fig. 4. Note that this sum decreases considerably slower in the cases with the secondary slip $\epsilon_{\xi\eta}^s$ than the case without. When this sum approaches zero, the extrusion approaches static extrusion and ceases to grow. The creep shear strain distributions $\epsilon_{\alpha\beta}^c$ in P and Q at different cycles of loading were calculated for the cases with and without secondary slip and are shown in Fig. 5. The $\epsilon_{\alpha\beta}^c$'s at the free surface versus cycles of loading n are shown in Fig. 6 this strain versus loading time N/f is shown in Fig. 7. Note that with no secondary slip, the extrusion growth ceases when the extrusion approaches the static extrusion. The creep strain $\epsilon_{\alpha\beta}^c$ in P and Q at the free surface, which represents the amount of extrusion or intrusion with the secondary slip is much higher than that without the secondary slip. Calculations also have been made at a frequency of loading of 10 cycles/min, and the creep strain in P and Q versus N/f have been found to be essentially the same as that at 345 cycles/min. In the high cycle range, the creep strain depends mainly on the time of loading. Similar calculations were made on a low frequency loading 0.345 cycles/min. The creep strain at this low frequency depends on the number of cycles as well as N/f the time of loading.

Conclusions

The amount of creep shear strains $\epsilon_{\alpha\beta}^c$ in P and Q at the free surface is a measure of the amount of extrusion and intrusion and, hence, is taken as a measure of fatigue crack initiation. The calculated results indicate that this surface creep strain depends only on the time of loading N/f in high frequency range and becomes dependent also on the number of loading cycles in the low frequency range.

Creep strain in the secondary slip system has a *tensor* component $\epsilon_{\alpha\alpha}^c$ which has the same effect in causing $\tau'_{\alpha\beta}$ in P and Q as $\tau'_{\alpha\alpha}$. Hence this creep strain $\epsilon_{\alpha\beta}^c$ in P and Q with this secondary slip is much larger than that without. Without the secondary slip, the extrusion ceases when it reaches the static extrusion. However, with the secondary slip, extrusion grows considerably beyond the static extrusion. This may be a main cause for the extent of extrusion to be much more in a face-centered polycrystal than that in a hexagonal polycrystal. The stress intensity factor of crack depends on the extent of extrusion on intrusion. Hence, this extent is important for the study of fatigue crack initiation.

Acknowledgments

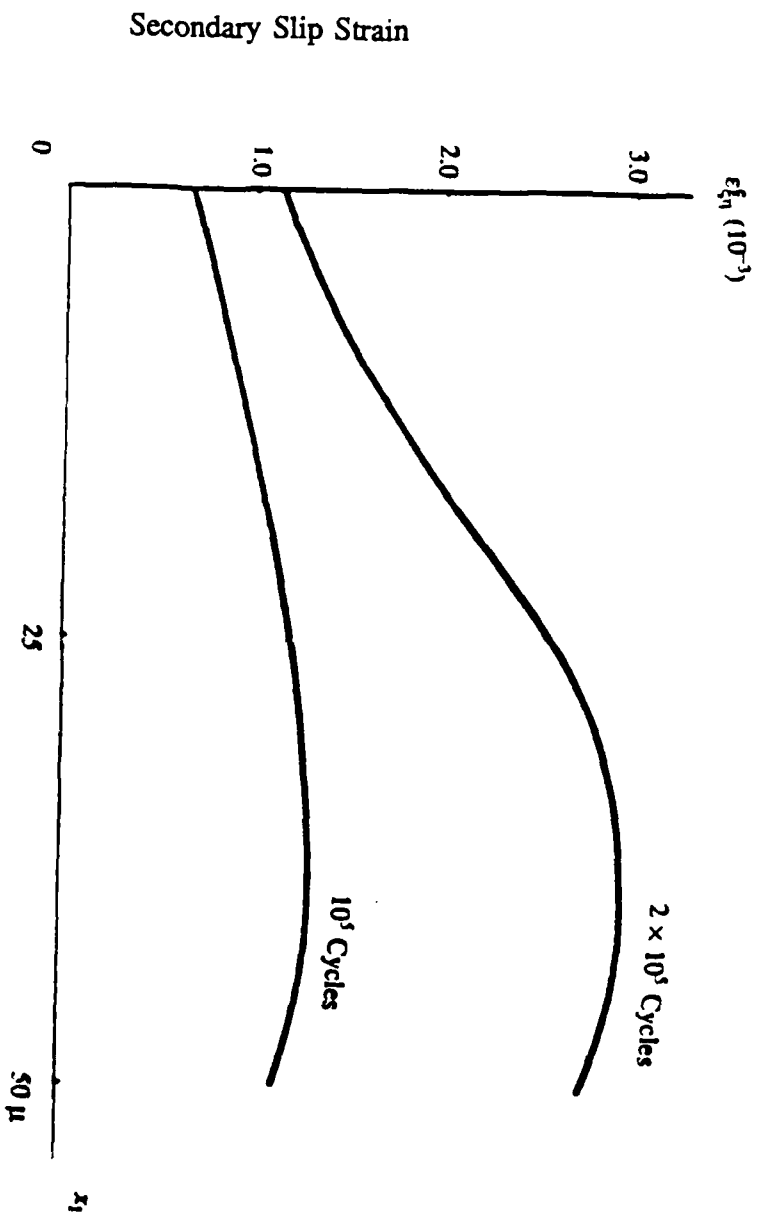
The support of the U.S. Office of Naval Research through Contract N00014-86-K-0153 and the interest of the scientific officer, Dr. Yapa Rajapakse, are gratefully acknowledge.

References

1. Cottrell, A.H. and D. Hull, "Extrusion and Intrusions by Cyclic slip in Copper", Proc. Roy. Soc. (London), Vol. 242A, p. 211, 1957.
2. Forsyth, P.J.E. and C.A. Stubbington, "The Slip Band Extrusion Effect Observed in Some Aluminum Alloys Subjected to Cyclic Stresses", J. Inst. Metals, Vol. 83, p. 395, 1955.
3. Frazer, R.A. W.J. Duncan and A.R. Collar, "Elementary Matrices and Some Applications to Dynamics and Differential Equations," Cambridge University Press, p. 45, 1938.
4. Gilman, J.J., "Micromechanics of Flow in Solids", McGraw-Hill, New York, pp. 176-179, 1969.
5. Johnson, R.D., R.R. Shober and A.D. Schope, "The Creep of Single Crystals of Aluminum", National Advisory Committee for Aeronautics, Technical Note 2945, 1953.
6. Johnson, R.D., A.P. Young and A.D. Schope, "Plastic Deformation of Aluminum Single Crystals at Elevated Temperatures", National Advisory Committee for Aeronautics, Technical Note 3351, 1955.
7. Kennedy, A.J. "Process of creep and Fatigue of Metals" John Wiley & Sons Inc. pp. 331-343, 1963.
8. Lin. T.H., "Micromechanic of Deformation of Slip Bands Under Monotonic and Cyclic Loadings", Reviews of the Deformation Behavior of Materials, P. Felham (ed.), Freund Publishing House; Tel-Aviv, Israel, 1977.
9. Lin. T.H., "Micromechanic of Fatigue Crack Initiation: Theory and Experimental Observation", Mechanics of Fatigue - AMD, Vol. 47, ASME, Edited by T. Mura, pp. 41-109, 1981.
10. Lin, T.H. and Y.M. Ito, "Mechanism of a Fatigue Crack Nucleation Mechanism," J. Mech. Phys. Solids, Vol. 17, pp. 511-523, 1969.
11. Lin, T.H. and S.R. Lin, "Micromechanics Theory of Fatigue Crack Initiation Applied to Time-Dependent Fatigue", ASTM STP 675, pp. 707-728, 1979.
12. Lin, T.H. and S.R. Lin, "Fatigue Crack Initiation with Creep" Defects and Fracture Edited by G-C. Shi and H. Zorski published by Martinus Nijhoff Publishers, pp. 3-13, 1982.
13. Lin, T.H., S.R. Lin and X.Q. Wu, "Micromechanics of an Extrusion in High-Cycle Fatigue" UCLA Engineering Rept. 88-09, 1988 and to be published in Philosophical Magazine.

14. McEviley, J., Jr. and E.S. Machlin, "Critical Experiments on the Nature of Fatigue in Crystalline Materials," Proc. Int. Conf. on the Atomic Mechanism of Fracture, Technology Press, MIT and John Wiley & Sons, 1959.
15. Mughrabi, H., R. Wang, K. Differt and U. Essmann, "Fatigue Crack Initiation by Cyclic Slip Irreversibilities in High-Cyclic Fatigue", Fatigue Mechanics, ASTM STP 811, pp. 5-45, 1983.
16. Mott, N.F., "Origin of fatigue Cracks", ACTA Metallurgica, Vol. 6, p. 195, 1958.
17. Parker, E.R., "*Theories of Fatigue*", *Mechanical Behavior of Materials in Elevated Temperatures*, Edited by J.E. Dorn, McGraw-Hill, pp. 129-148, 1961.
18. Taylor, G.I., "Plastic Deformation of Metals", J. Inst. Metals, Vol. 62, p. 307, 1938.
19. Thompson, N., N.J. Wadsworth and N. Louat, "The Origin of Fatigue Fracture in Copper," Phil. Mag., Vol. 1, p. 113, 1955.
20. Thompson, N., "Proc., Int. Conf. on the Atomic Mechanism of Fracture, Technology Press MIT and John Wiley & Sons, 1959.
21. Wood, W.A., *Mechanism of Fatigue*," Fatigue in Aircraft Structures (Edited by A.M., Freundental), Academic Press, New York, 1956, pp. 1-19.

Loading: 345 c.p.m.



Distance from Free Surface

Figure 3. Creep Strain Distribution of Secondary Slip

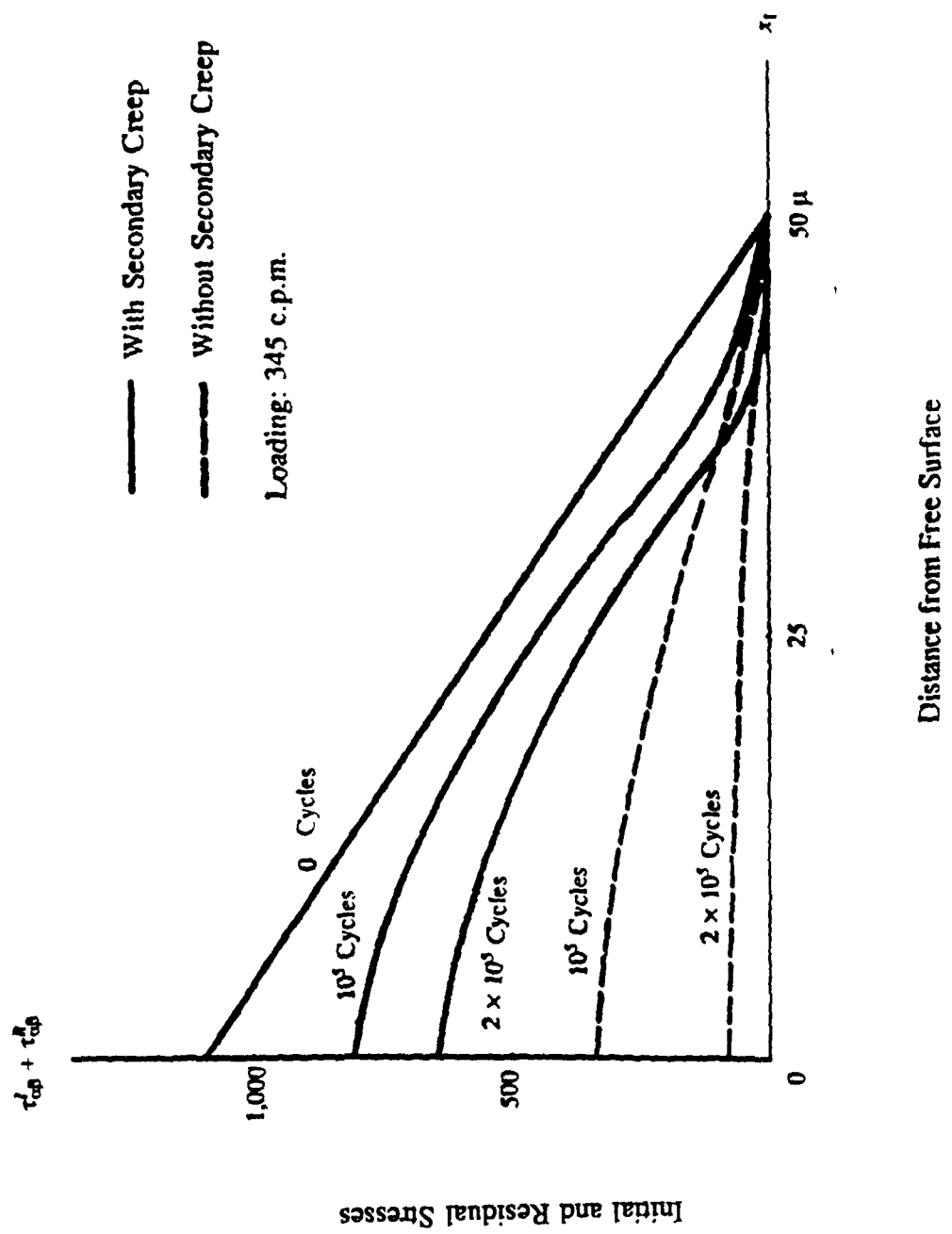


Figure 4. Initial and Residual Stress Distribution in P and Q (P and Q Opposite Sign)

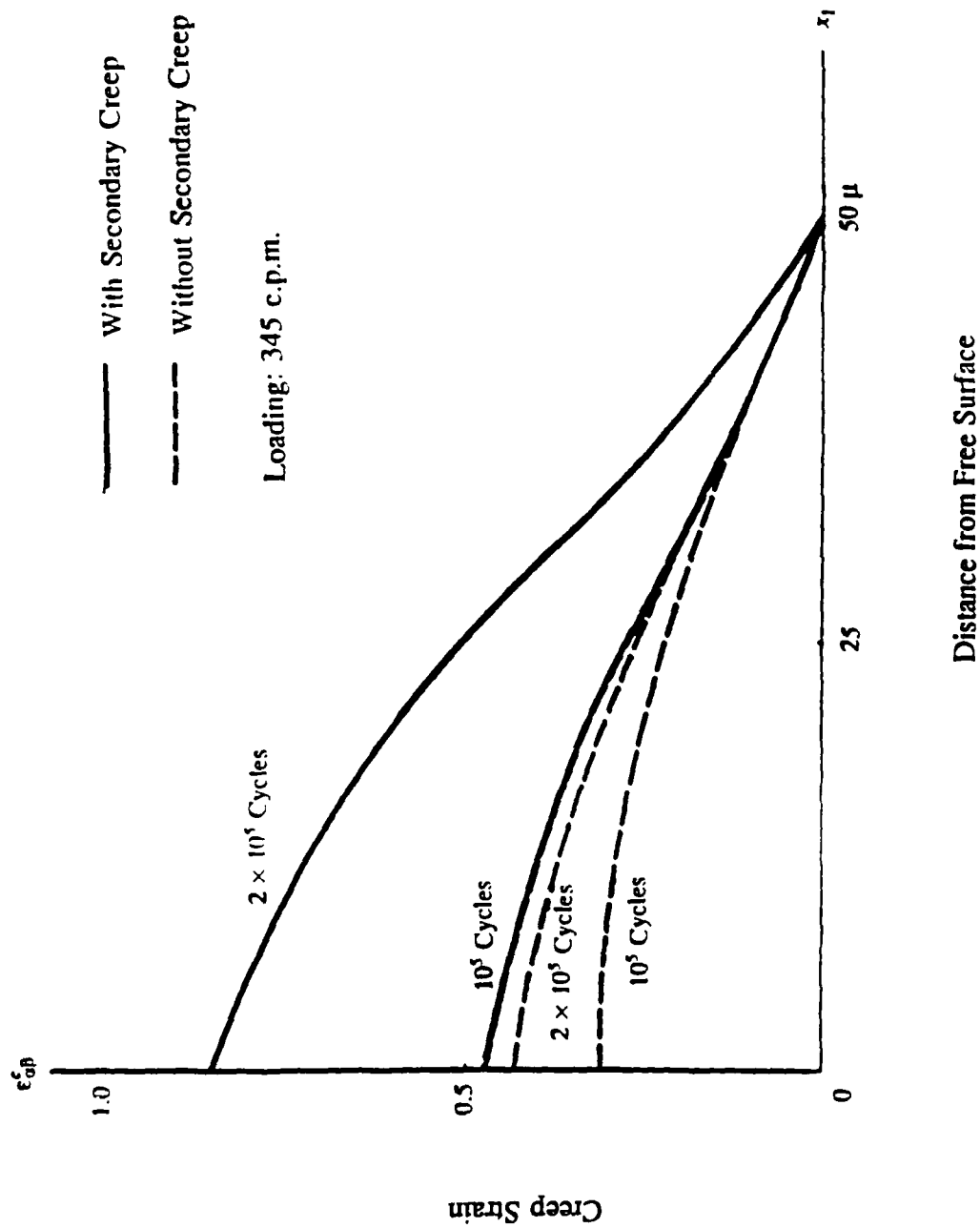


Figure 5. Creep Strain Distribution

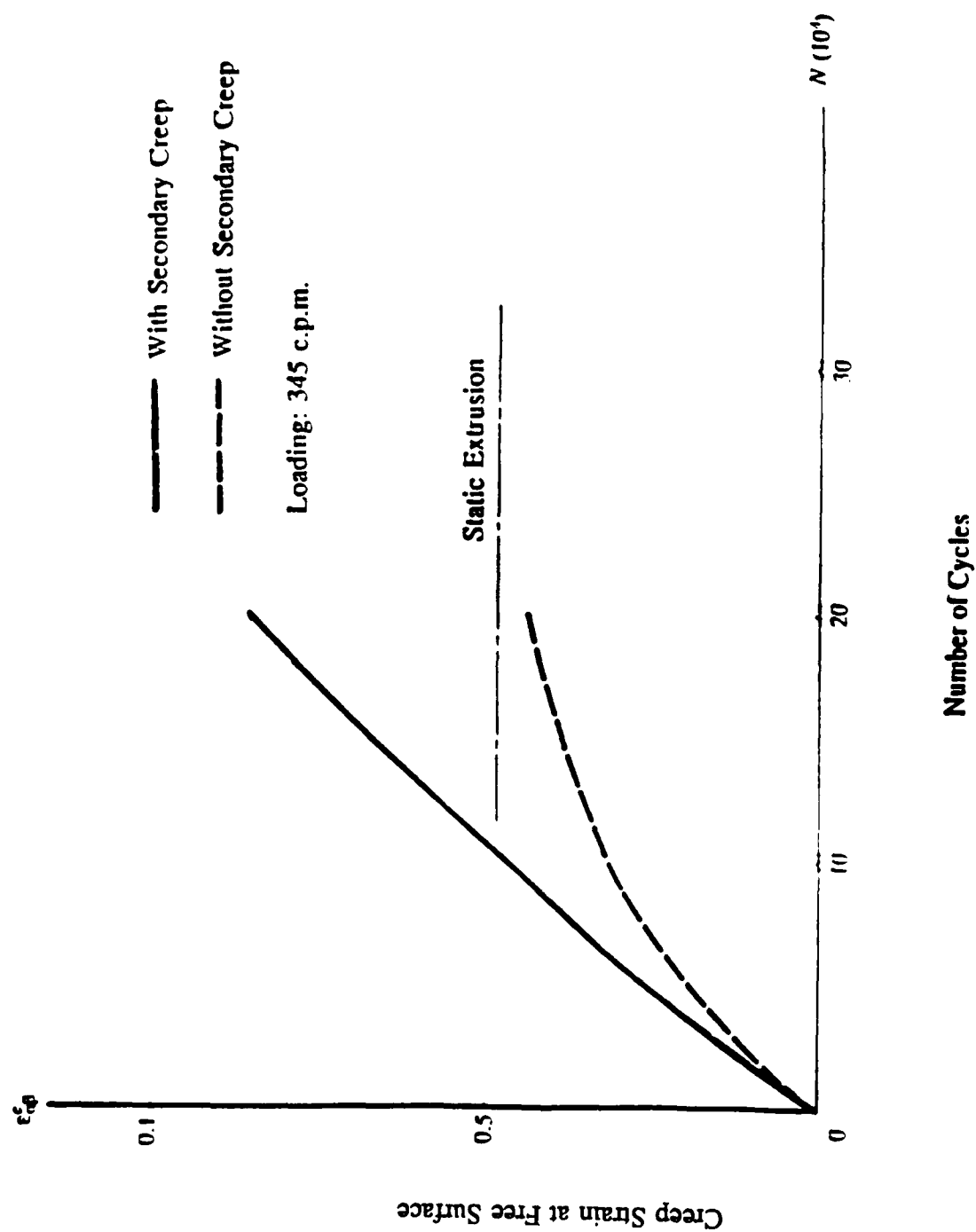


Figure 6. Creep Strain at Free Surface versus Number of Cycles

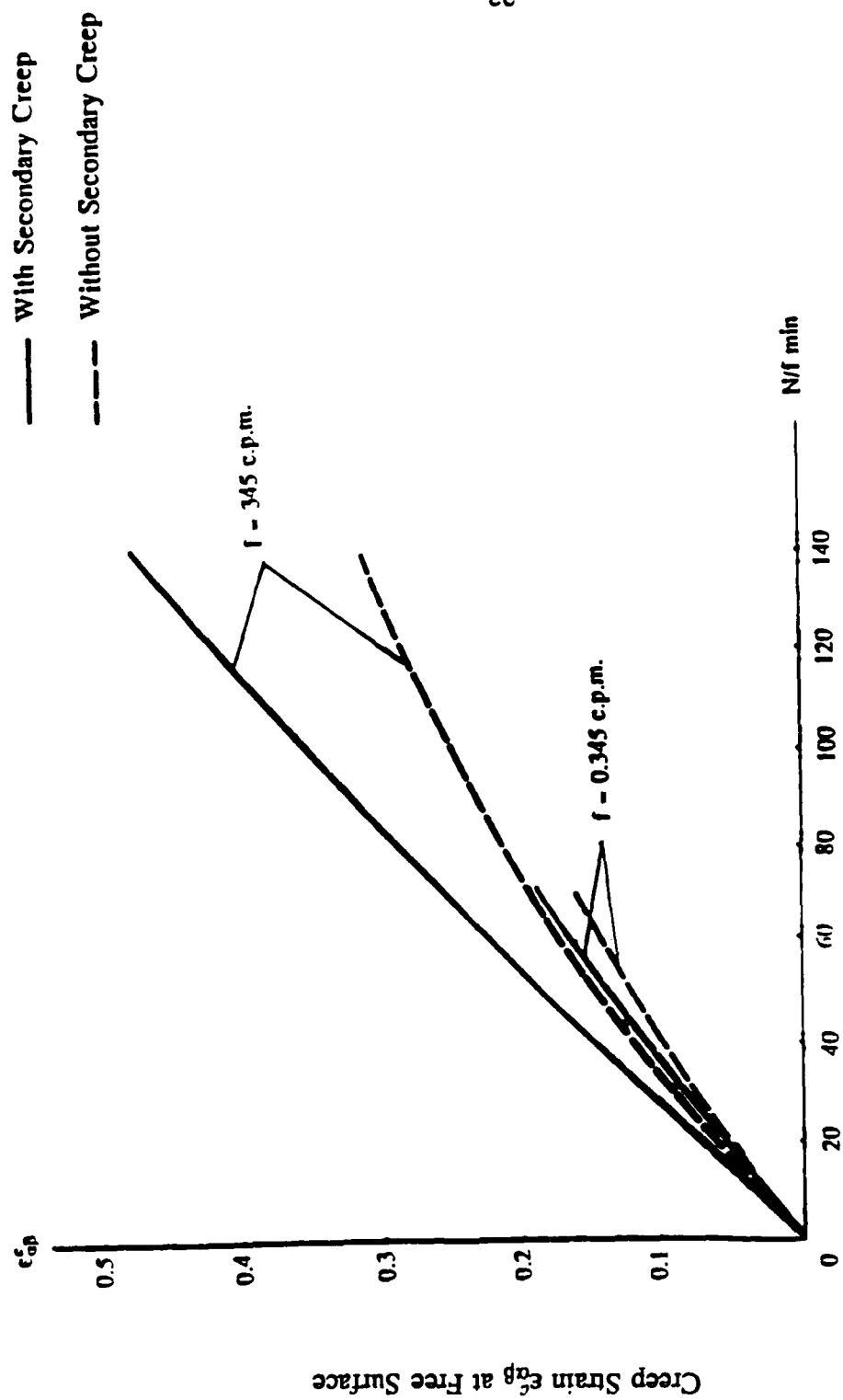


Figure 7. Creep Strain Buildup at Free Surface versus Loading Time N/f